The absorption spectrum of ammonia between 5650 and 6350 cm−1

P. Cacciani, P. Čermák, S. Béguier, A. Campargue

Version of Record: https://www.sciencedirect.com/science/article/pii/S0022407320306816
Manuscript_33d0af9109cd4d3090399b2ac85e9008

The absorption spectrum of ammonia between 5650 and 6350 cm^{-1}

P. Cacciani [1], P. Čermák [2], S. Béguier [3] and A. Campargue [3] *

[1] *Univ. Lille, CNRS, UMR 8523 - PhLAM - Physique des Lasers, Atomes et Molécules, 59000 Lille, France*
[2] *Department of Experimental Physics, Faculty of Mathematics, Physics and Informatics, Comenius University, Mlynská dolina F2, 842 48 Bratislava, Slovakia*
[3] *Univ. Grenoble Alpes, CNRS, LIPhy, 38000 Grenoble, France*

Number of pages: 18
Number of tables: 1
Number of figures: 9

17 December 2020

Key words: Ammonia; NH3; Transparency window; HITRAN

* Corresponding author: Alain.Campargue@univ-grenoble-alpes.fr

Abstract

A room temperature Fourier Transform absorption spectrum of ammonia measured in 1991 and available from the Kitt Peak data center is analyzed in the 5650 - 6350 cm^{-1} region. This spectral interval is part of the important 1.6 μm atmospheric transparency window where ammonia could be detected as trace species. The centers and intensities of 2779 ammonia lines were retrieved using a multiline fitting procedure. The spectrum was assigned by the joint use of a recent variational line list and of lower state combination difference relations. Overall, 1762 lines were assigned to 29 bands providing 914 new experimental energies. The assignments and upper state experimental energies presented in this work are the first for ammonia in the studied region. The comparison of our line list to the variational line list, to the HITRAN2016 list and to a very recent experimental line list is presented and discussed.

1. Introduction

The present study originates from the difficulty of identifying a number of very weak lines detected in high sensitivity spectra of water vapor recorded near 1.6 µm by cavity ring down spectroscopy (CRDS) at low pressure [1–3]. In these experiments, the achieved detectivity threshold of the water line intensities was on the order of 10^{-29} cm/molecule. That made visible absorption lines of trace species with very low relative abundances, *e.g.*, some tens ppb relative concentration in the case of ammonia. The identification of these ammonia lines was made difficult by the fact that *(i)* their intensities scaled according to water lines (as NH_3 was present in the water sample used to fill the CRDS cell), *(ii)* their line profile at low pressure was very close to that of the water lines (as a consequence of the similar values of the molecular masses, Doppler broadenings are very close in H_2O and NH_3), and *(iii)* the absence of an accurate line list of ammonia available in the literature for the considered spectral region. Finally, ammonia lines could be identified by direct comparison with an absorption spectrum of pure ammonia recorded by Fourier transform spectroscopy (FTS) at the Kitt Peak National Solar Observatory available in open access. The present work is devoted to the line list construction and assignment of this NH_3 spectrum in the 5650- 6350 cm^{-1} region. The investigated region is presented on the overview spectrum of ammonia between 5000 and 10000 cm^{-1} in **Fig. 1**.

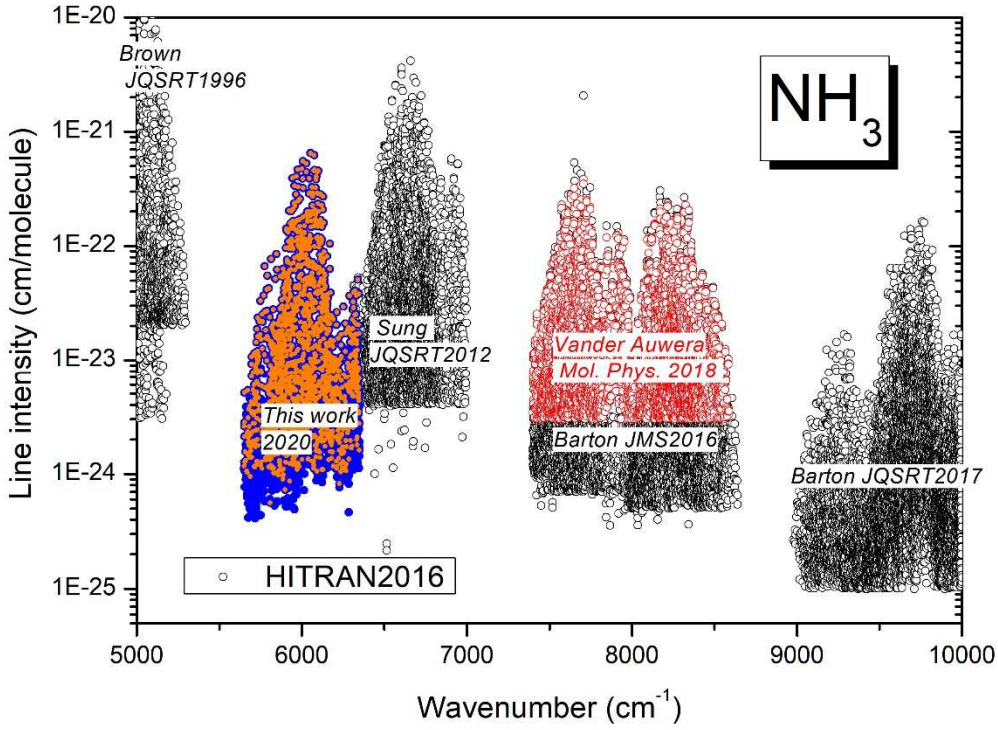

Fig. 1

Overview of the NH_3 spectrum between 5000 and 10000 cm^{-1}. The primary sources of the HITRAN2016 line list [4] (black) are indicated: Brown et al. [5], Sung et al. [6] and Barton et al. [8]. An accurate line list has been recently released by Vander Auwera and Vanfleteren for the 7400–8640 cm^{-1} region [9] (red). The orange symbols mark the assigned transitions of the line list presently generated in the 5650–6350 cm^{-1} interval (blue circles).

In recent years, significant experimental progress has been performed to improve the knowledge of the near-infrared ammonia spectrum. The HITRAN2016 line list [4] reproduces the results of the analysis of two FTS spectra of the Kitt Peak archive in the 7400-8640 cm^{-1} [7] and 8800-10400 cm^{-1} [8] regions. A higher-quality line list has been recently released by Vander Auwera and Vanfleteren for the first region [9]. In the 1.5 μm region (6300-7000 cm^{-1}), the HITRAN2016 list uses as main source the FTS line parameters by Sung et al. [6]. This region of strong absorption was the subject of several studies aiming to extend the rovibrational assignments [10–14]. In particular, the empirical determination of the lower state energy was performed using the temperature dependence of the line intensities in the cooled Herriott cell (122-300 K) [10,11] and in the jet expansion (20-80 K) [12,13]. Very recently, Beale et al. [14] reported FTS line lists of ammonia at elevated temperatures (293-900 K at 100 K intervals) and pressures of 10 Torr and 100 Torr for the broad 4800-9000 cm^{-1} region, thus including the region of our interest. Part of the transitions were reported with empirical values of the lower state energy.

On the theory side, extended variational line lists have been recently made available by Huang et al. [15,16] using an experimentally refined potential energy surface to obtain energies and quantum assignments, and by the UCL group who generated the BYTe [17] and C2018 [18] *ab initio* line lists. As a rule, the *ab initio* line positions do not have experimental accuracy. They can be improved by adjusting variational positions according to empirical values of the lower and upper energy levels. The MARVEL spectroscopic networks approach [19] has been recently applied to experimental line lists of ammonia up to 17000 cm^{-1} in order to provide an extensive set of empirical energy levels for the main isotopologue, $^{14}NH_3$ [20]. Subsequently, Coles et al. [21] used these levels to improve the accuracy of the C2018 list creating a new semi-empirical “CoYuTe” list, which is currently recommended for ammonia by the ExoMol database. Let us note that according to the exhaustive review of available experimental sources included in Ref. [20], the present study, and the above-mentioned lists of Beale et al. [14], reported without rovibrational assignment, are the first ones in the 5650-6350 cm^{-1} region.

The rest of the paper is organized as follows. After the presentation of the FTS spectrum under analysis and of the line list construction (section 2),

rovibrational assignments performed based on the theoretical lists and supported by the extensive use of lower state combination difference relations are presented in section 3 together with a systematic comparison to the C2018 line list. Finally, section 4 contains a conclusion, including the comparison with line lists provided in the HITRAN2016 [4] database and those reported by Beale et al. [14].

2. Experimental data

2.1. The Kitt Peak spectrum

The room temperature absorption spectrum of NH_3 under analysis (910606R0.016) was recorded in June 1991 using the FTS spectrometer on the McMath Solar Telescope which was located at Kitt Peak National Solar Observatory. The spectrum covering the 3000-8000 cm^{-1} range was acquired with a pressure of pure ammonia of 1.8 Torr and an absorption pathlength of 16 meters. The spectral resolution was about 0.01 cm^{-1}, and the estimated temperature value was 21.5 °C.

2.2. Construction of the line list

The wavenumber scale of the spectrum was calibrated using ammonia lines near 6300 cm^{-1} listed in the HITRAN2016 database. Lines due to water vapor, present as an impurity, are present near 5700 cm^{-1} and were used for verification of the obtained frequency calibration. We estimate the accuracy of the frequency scale to be 2×10^{-3} cm^{-1}.

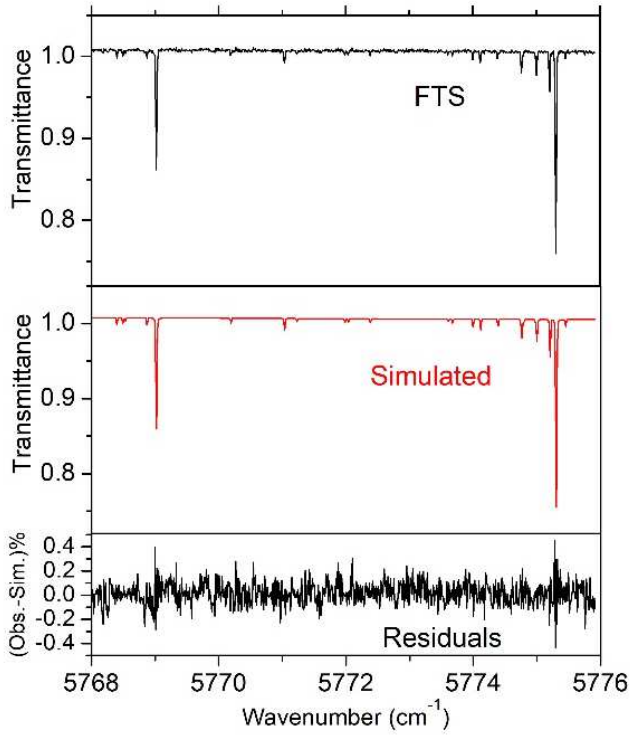

Fig. 2

Illustration of the multiline fitting procedure adopted to retrieve the ammonia line parameters. The FTS spectrum (910606R0.016) was recorded at Kitt Peak National Solar Observatory with a pressure of ammonia of 1.8 Torr and an absorption pathlength of 16 meters.

The line centers and line intensities were retrieved using a multiline fitting of the spectrum based on a homemade three-step suite of programs written in Labview and C++ (see Refs. [22] for details). After correction of the baseline, a peak finder procedure is used to construct a preliminary peak list (line center, peak height). A synthetic spectrum is then simulated by attaching to each peak a default Voigt profile determined from a small number of isolated lines (the Gaussian and Lorentzian default widths are average values and include the contribution of the instrument function that is not modelled). Then an automatic multiline fit is performed over the entire analyzed region by adjusting the line center and integrated line absorbance, the shape of all the lines being fixed to the default Voigt profile. Finally, a manual adjustment is performed by refining the profile parameters (when needed) and adding/deleting weak lines. **Fig. 2** illustrates the quality of the achieved spectrum reproduction. The *rms* deviation of the differences between the measured and simulated transmittances is about 0.1% which, taking into account the 16 m absorption path length, corresponds to a noise equivalent absorption coefficient of $\alpha_{min} \approx 6\times10^{-7}$ cm^{-1} leading to a detectability threshold of about 10^{-24} cm/molecule in terms of line intensities.

After the removal of some water lines located at the low energy edge of the studied spectral region, the overall list, presented in **Fig. 1**, includes 2779 lines with intensities ranging between about 10^{-24} and 10^{-21} cm/molecule. The average uncertainty on the retrieved line intensities is estimated to be on the order of 5-10 % for isolated lines of intermediate intensity. Comparison to HITRAN intensity values for a sample of lines on the high energy edge of the spectrum around 6300 cm^{-1} shows a systematic difference on the order of 10%, which is discussed in section 4. Overall, the accuracy of the reported line positions is estimated to be on the order of 3×10^{-3} cm^{-1} for isolated lines.

3. Spectrum analysis

3.1. Assignments

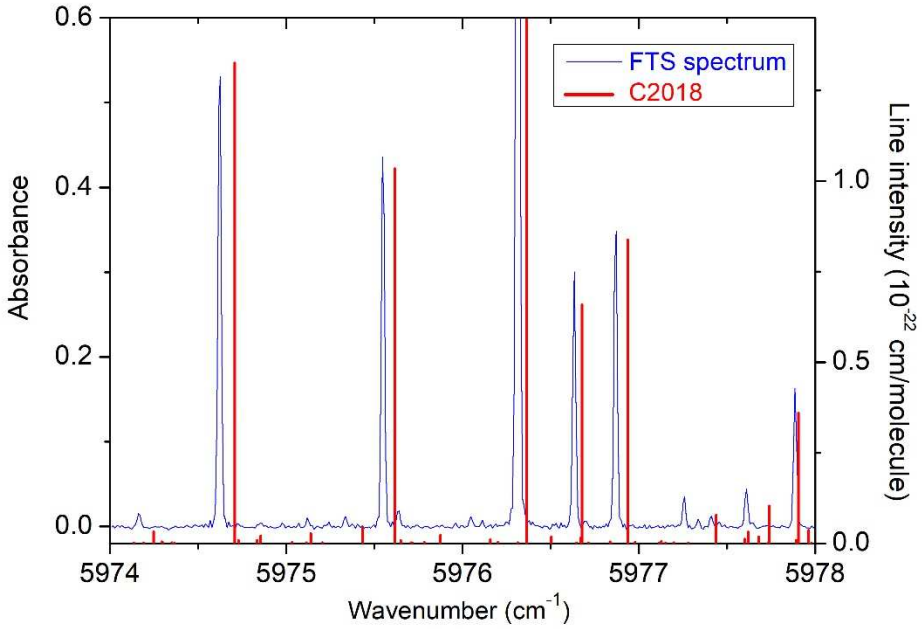

Fig. 3.
Comparison between the FTS and calculated C2018 line lists of $^{14}NH_3$ [18] around 5976 cm^{-1}.

To perform the rovibrational assignment of the experimental line list, we used the improved version of the BYTe – the C2018 list as reference list [18]. In this region, the C2018 list is practically identical to the semi-empirical CoYuTe list, both available on the EXOMOL website [www.exomol.com]. As shown in **Figs. 3 and 4**, the C2018 line list shows a remarkable similarity to the experimental data. Let us mention that the labeling of the states follows the conventions of the C2018 list where 13 quantum numbers represent each energy level: υ_1, υ_2, υ_3, υ_4, L_3, L_4, *inv*, $\Gamma_{vib.}$, *J*, *K*, $\Gamma_{rot.}$, N_B, $\Gamma_{tot.}$ where υ_i are the vibrational normal-mode quantum numbers corresponding to the υ_1 symmetric stretch, υ_2 symmetric bend, υ_3 the antisymmetric stretch, υ_4 antisymmetric bend, respectively. $L_3=|l_3|$ and $L_4=|l_4|$ are the corresponding vibrational angular momentum quantum numbers, *inv=a/s* is the inversion symmetry (asymmetric/symmetric or odd/even), and $\Gamma_{vib.}$ is the symmetry of the vibrational motion. *J* is the total angular-momentum quantum number, $K=|k|$ is the projection of the total angular momentum on the molecule-fixed axis z, and $\Gamma_{rot.}$ is the rotational symmetry. Finally, $\Gamma_{tot.}$ stands for the full symmetry of the eigenstate, and N_B is the block counting number used during the generation of the C2018 list.

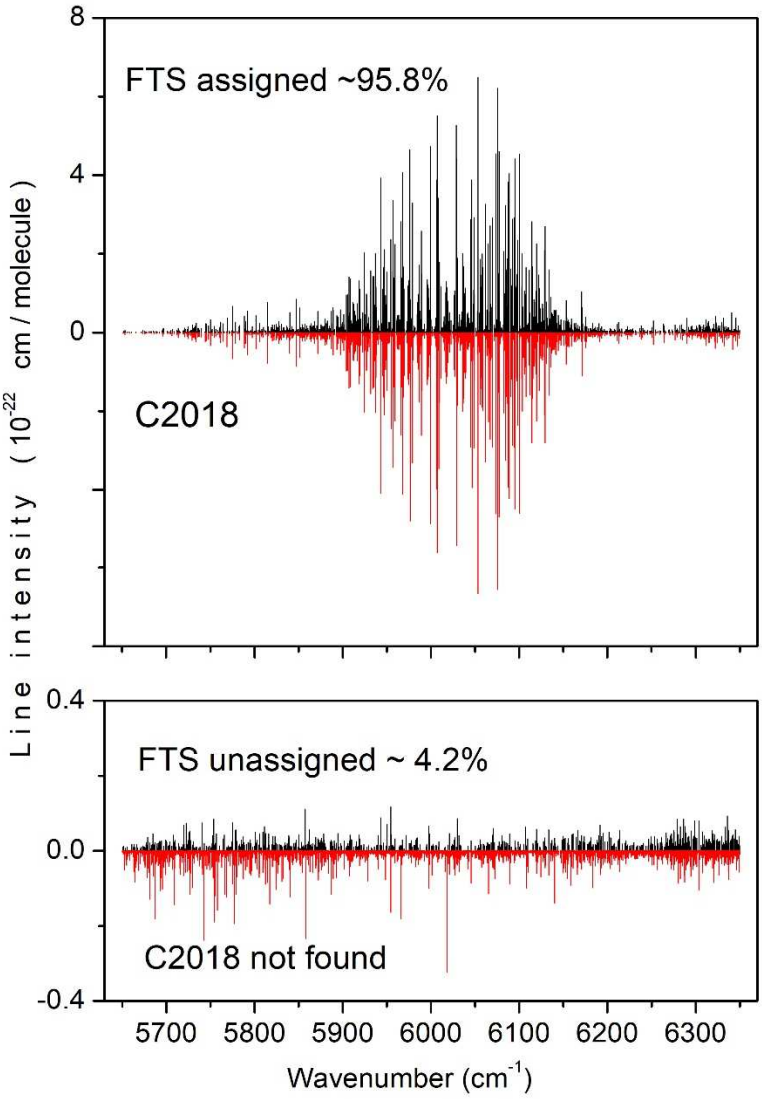

Fig. 4.
Comparison between the FTS and calculated C2018 line lists of $^{14}NH_3$ [18].
Upper panel: assigned and C2018 corresponding transitions (black and red, respectively)
Lower panel: unassigned experimental transitions (black) and C2018 transitions not identified in the FTS spectrum list (red).

In a first step, for each line, the best corresponding C2018 candidates were selected using as a criterion the agreement of both the line center and line intensity. Typically, around ten candidates were found for a position agreement within 1.5 cm^{-1} and an intensity agreement within a factor of two. The second step consisted in verification of these possible assignments by a lower state combination difference (LSCD) process. For each candidate transition, its upper state energy was calculated by adding the lower state energy taken from an accurate list constructed by Cacciani et al. [23] for ammonia ground and υ_2 state. Then the transitions with the same upper state level were identified in the C2018 list, and their frequency was adjusted using the newly calculated upper state of the candidate transition. Using the C2018 intensity, we looked for these "CD" lines not only inside our line list but also among the lines present in the HITRAN2016 and in Beale's room temperature 10

Torr list. The combination transition was considered as existing if an experimental line was found in one of the line lists within typically ±0.006 cm^{-1} from the calculated position with a maximum intensity difference of a factor of 2. This relatively large criterion of 0.006 cm^{-1} originated from the fact that the spectrum resolution was limited to 0.01 cm^{-1} and the sampling step had a similar value leading to the absorption line profile defined by no more than 5 points. Finally, the assignment was considered validated when multiple CD transitions were found. Some upper state determinations were supported by up to six transitions, which added to the accuracy of the determined energy value. At the opposite end, some of our assignments could not be supported by LSCD relations. In those cases, the smooth variation of the (obs.-calc.) upper state energy value within the given vibrational band was applied to support the assignment. **Figure 5** illustrates how this criterion was applied to the $\nu_1+3\nu_2$ (a) parallel vibrational band. The C2018 upper energy levels are plotted as a function of *J+K/(J+1)*. The upper levels with experimental determination are highlighted, and the corresponding (obs.-calc.) deviations are presented on the lower panel. Such kinds of band overview were valuable to assign transitions reaching new upper state levels, using guessed values of the (obs.-calc.) deviations to correct the C2018 line positions.

Overall, 1762 transitions belonging to 29 bands could be assigned (see **Figs. 1 and 4**). The complete list of experimental transitions with their assignment, when available, and corresponding C2018 position and intensity values is provided as a Supplementary Material. On the lower panel of **Fig. 4**, we have plotted the lines left unassigned in the experimental spectrum together with those of the C2018 list for which we could not find their experimental counterpart. This figure shows that all the lines with large or intermediate intensities were assigned. The unassigned lines have an intensity less than 10^{-23} cm/molecule (to be compared to maximum intensity value of more than 6×10^{-22} cm/molecule) and represent no more than 4% of the total experimental intensity in the considered 5650-6350 cm^{-1} range (note that minor isotopologues were not considered in the analysis - they are expected to bring about 0.4% of the intensity in the region).

The band-by-band statistics is presented in **Table 1,** which includes intensity information and comparison with the corresponding C2018 values. The dominant band, $(\nu_2+\nu_3+\nu_4)$ L_3=1 L_4=1 (E symmetry), is almost completely assigned (transitions bringing 98% of C2018 integrated intensity are assigned), and a percentage of more than 80% is reached for five other vibrational bands. We note the poor assignment of the $\nu_2+3\nu_4$, L_4 = 1 band, which according to the C2018 list, is the fifth in the intensity ranking of the bands contributing in the considered spectral range. Only one line could be reliably assigned. The superposition of the stick spectrum of the experimental lines left unassigned to the C2018 $\nu_2+3\nu_4$, L_4 = 1 band indicates that the strongest C2018 intensities of this band are significantly larger than the strongest unassigned lines. This observation questions the quality of the C2018 intensities of the considered bending band.

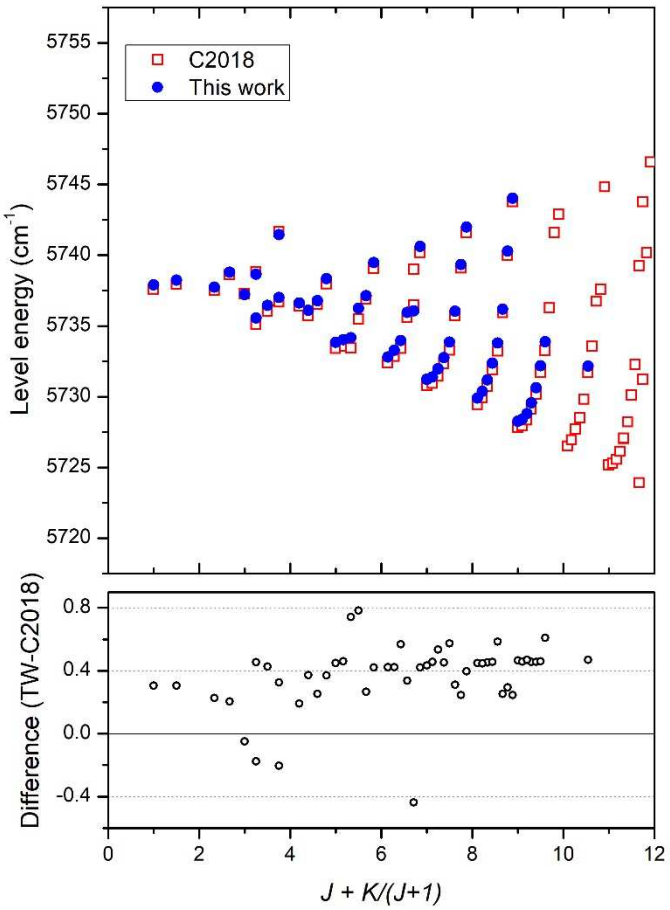

Fig. 5.

Comparison of the experimental and C2018 values (red and blue symbols, respectively) of the upper state energy term values for the $\nu_1+3\nu_2$ (a) vibrational band. For the sake of clarity, the average rotational term ($9.6J(J+1)-3.6K^2$) was subtracted from each energy value. On the lower panel, the (Exp.-C2018) position differences are presented. Some sequences of deviations show a smooth variation *versus* $J+K/(J+1)$, which helped to extend the assignments (so-called "branch criterion" method).

From the 1762 assigned transitions in the 5650-6350 cm^{-1} range, 916 upper state energies could be derived. According to the MARVEL list [20], only two of them were already known. The list of energy levels provided as Supplementary Material is sorted by vibrational quantum numbers and vibrational symmetry. A standard deviation is provided for the upper state energies derived from more than one transition. Note that typical uncertainty values on the energy levels determined from various transition frequencies are on the order of 0.002 cm^{-1}.

Table 1: Statistics and integrated absorption of the various vibrational bands contributing to the $^{14}NH_3$ spectrum between 5650 and 6350 cm^{-1}. The bands are ordered according to their C2018 integrated intensities. All the bands with C2018 integrated intensities larger than 3×10^{-23} cm/molecule are listed.

Vibrational band	Upper state [a]	C2018			This work			Int. ratio [h] %	$<\delta>$ [i] (cm^{-1})
		E_0 [b] (cm^{-1})	Nb [c]	Band Int. [d] (cm/molecule)	Nb [e]	J_{min}/J_{max} [f]	Band Int. [g] (cm/molecule)		
$\nu_2+\nu_3^1+\nu_4^1$ (E') s	011111	6012.9	768	1.92E-20	345	0/15	1.89E-20	**98.6**	-0.05
$\nu_2+\nu_3^1+\nu_4^1$ (E'') a	011111	6036.5	810	1.83E-20	328	0/16	1.79E-20	**98.0**	-0.08
$3\nu_2+\nu_3^1$ (E') s	031010	5856.1	594	3.00E-21	221	0/13	2.73E-21	**91.7**	0.15
$3\nu_2+\nu_3^1$ (E'') a	031010	6331.3	248	8.56E-22	68	0/9	6.53E-22	**78.5**	0.11
$\nu_2+\nu_3^1+\nu_4^1$ (A_2'') a	011111	6049.6	338	1.11E-21	100	0/10	9.05E-22	**82.9**	-0.21
$\nu_2+\nu_3^1+\nu_4^1$ (A_1'') a	011111	6033.7	338	8.83E-22	84	2/9	7.68E-22	**78.5**	-0.18
$\nu_2+\nu_3^1+\nu_4^1$ (A_1') s	011111	6024.3	295	8.70E-22	78	1/9	6.17E-22	**76.5**	-0.29
$\nu_2+\nu_3^1+\nu_4^1$ (A_2') s	011111	6008.0	265	6.98E-22	48	3/8	5.68E-22	**81.6**	-0.24
$4\nu_4^2$ (E') s	000402	6372.6	234	6.88E-22	53	1/9	5.75E-22	**76.5**	-0.73
$4\nu_4^2$ (E'') a	000402	6375.6	160	4.36E-22	33	1/9	3.51E-22	**74.2**	-1.04
$\nu_2+3\nu_4^1$ (E'') a	010301	5755.6	307	5.49E-22	0	-	-	-	-
$\nu_2+3\nu_4^1$ (E') s	010301	5682.6	249	4.64E-22	1	5/5	1.33E-24	**0.3**	-0.35
$\nu_1+\nu_2+\nu_4^1$ (E'') a	110101	5930.8	355	5.33E-22	84	0/11	4.26E-22	**66.5**	-0.31
$\nu_1+\nu_2+\nu_4^1$ (E') s	110101	5897.8	315	2.82E-22	42	1/10	1.65E-22	**46.8**	-0.40
$\nu_1+3\nu_2$ (A_1') s	130000	5737.9	153	5.25E-22	70	1/10	3.88E-22	**88.9**	0.35
$\nu_1+3\nu_2$ (A_2'') a	130000	6230.3	137	1.96E-22	38	0/9	1.22E-22	**63.2**	0.59
$2\nu_2+\nu_3^1+\nu_4^1$ (E') s $\leftarrow\nu_2$	021111	5784.8	248	4.99E-22	74	0/9	3.41E-22	**68.2**	-0.18
$2\nu_2+\nu_3^1+\nu_4^1$ (E'') a $\leftarrow\nu_2$	021111	5984.9	257	3.45E-22	41	1/7	1.86E-22	**51.5**	-0.11
$4\nu_4^4$ (E'') a	000404	6432.0	129	1.35E-22	10	4/6	6.28E-23	**42.7**	-0.39
$4\nu_4^4$ (E') s	000404	6429.5	128	1.33E-22	6	4/10	2.29E-23	**18.1**	0.09
$6\nu_2$ (A_1') s	060000	6043.4	57	1.27E-22	5	8/9	9.69E-23	**71**	-0.02
$2\nu_2+3\nu_4^3$ (A_1') s	020303	6348.8	168	1.11E-22	6	3/7	2.18E-23	**17.4**	-0.61
$2\nu_2+3\nu_4^3$ (A_2') s	020303	6350.8	61	3.79E-23	2	5/5	7.52E-24	**11.6**	0.36
$3\nu_2+2\nu_4^2$ (E'') a	030202	6155.1	170	9.15E-23	0	-	-	-	-
$4\nu_4^0$ (A_2'') a	000400	6356.2	98	8.79E-23	6	2/7	3.26E-23	**34.6**	-1.23

$3\nu_2 + 2\nu_4^0$ (A$_2$'') a	030200	6133.6	130	7.82E-23	3	9/10	3.34E-23	**30.5**	0.27
$4\nu_2 + \nu_4^1$ (E'') a	040101	5708.3	107	7.51E-23	0	-	-	-	-
$2\nu_2 + 3\nu_4^1$ (E') s	020301	6314.1	130	6.51E-23	0	-	-	-	-
$\nu_2 + 3\nu_4^3$ (A$_2$') s	010303	5717.8	94	6.35E-23	0	-	-	-	-
$\nu_2 + 3\nu_4^3$ (A$_2$'') a	010303	5788.7	93	3.65E-23	0	-	-	-	-
$\nu_2 + 3\nu_4^3$ (A$_1$') s	010303	5718.7	43	3.27E-23	0	-	-	-	-
$\nu_1 + \nu_3^1$ (E'') a	101010	6609.8	67	6.04E-23	4	9/11	2.19E-23	**31.6**	0.01
$\nu_1 + \nu_3^1$ (E') s	101010	6608.8	71	5.26E-23	2	9/10	1.16E-23	**20.8**	0.02
$5\nu_2 + \nu_4^1$ (E') s	050101	6355.5	49	5.48E-23	3	5/6	2.42E-23	**35.2**	-0.58
$\nu_1 + 2\nu_4^2$ (E') s	100202	6556.4	48	3.74E-23	2	9/10	1.15E-23	**30.2**	0.22
$4\nu_2 + \nu_3^1$ (E') s $\leftarrow \nu_2$	041010	5945.7	103	3.28E-23	0	-	-	-	-
$2\nu_1$ (A$_2$'') a	200000	6520.6	64	3.04E-23	4	8/9	5.87E-24	**15.8**	-0.01
Sum [j]				**5.08E-20**	**1762**		**4.59E-20**		
Others [k]				2.79E-22	1017		1.84E-21		
Total [l]				**5.11E-20**	**2779**		**4.77E-20**		

Notes

[a] Vibrational labelling: $V_1V_2V_3V_4L_3L_4$ where $V_{i=1-4}$ are the vibrational normal mode quantum numbers corresponding to the ν_1 symmetric stretch, ν_2 symmetric bend, ν_3 the antisymmetric stretch, ν_4 antisymmetric bend, respectively. $L_3=|l_3|$ and $L_4= |l_4|$ are the vibrational angular momentum quantum numbers of the ν_3 and ν_4 modes, respectively.

[b] Energy of the lowest level of the upper vibrational state (corresponding generally to $J=K=0$) as calculated in the C2018 list [18]. In the case of the hot bands, the $J=K=0$ value of the lowest state was subtracted.

[c] Number of lines of the corresponding band with C2018 intensity larger than 1×10^{-25} cm/molecule.

[d] Sum of the C2018 intensities larger than 1×10^{-25} cm/molecule

[e] Number of lines of the corresponding band assigned in the studied spectrum

[f] Minimum and maximum values of the rotational quantum numbers of the assigned lines

[g] Sum of the experimental intensities of the considered band

[h] Ratio of the sum of the C2018 intensities of the transitions identified in the studied spectrum by the total C2018 intensity of the considered band.

[i] Average value of the (exp.- C2018) position differences of the considered band

[j] Sum of the intensities of the listed bands

[k] For the experimental list of transitions, "others" correspond to the intensity sum of the unassigned transitions while for the C2018 line list, it corresponds to the total intensity of the predicted vibrational bands with intensity smaller than smallest observed band.

[l] Sum of the two above values corresponding to the total C2018 intensity (intensity cut off of 1×10^{-25} cm/molecule) and all the measured absorption lines.

3.2. Comparison to the C2018 list

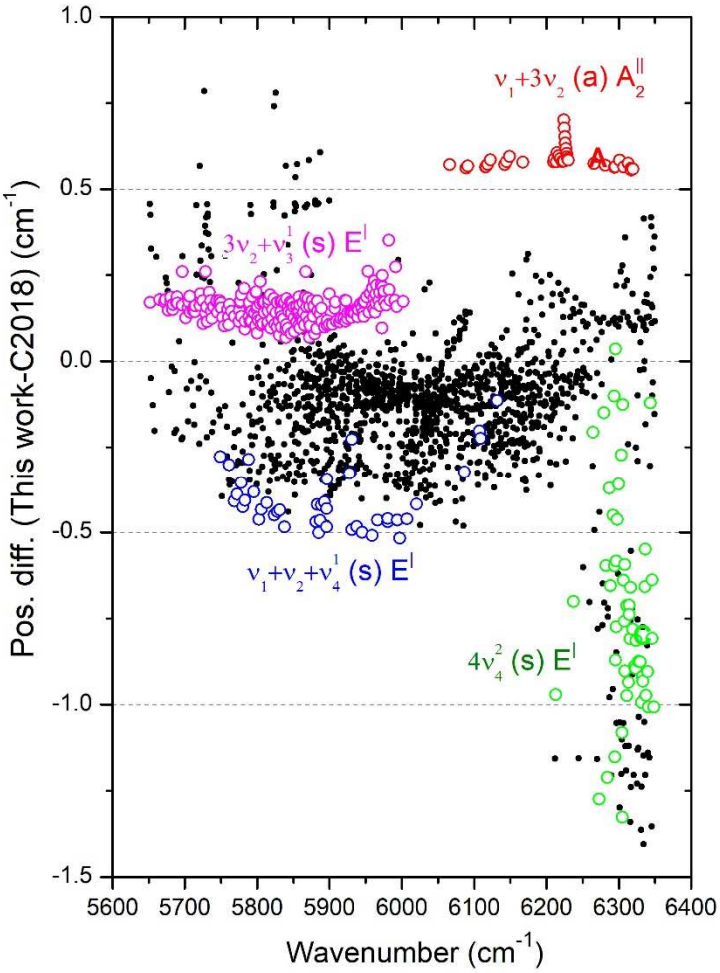

Fig. 6.
Overview of the (Exp. – C2018) position differences of the $^{14}NH_3$ lines assigned between 5650 and 6350 cm^{-1}. In general, the deviations depend mostly on the vibrational band and have a limited rotational dependence as illustrated by three of the four bands highlighted.

The differences between the measured and C2018 position values are presented in **Fig. 6.** Depending on the vibrational band, deviations range between -1.5 and 0.7 cm^{-1} (see average deviation values included in **Table 1**). The deviations relative to four bands are highlighted to illustrate the fact that, in general, the rotational dependence is limited within a given band.

Fig. 7 shows the Exp/C2018 intensity ratio *versus* the FTS line intensity of the assigned lines. The overall agreement is very good with an average value of 1.03 and an *rms* of 0.28 to be compared to the experimental estimated error bar of 10 % on the intensities. In particular, the strongest lines (belonging to the $\nu_2+\nu_3+\nu_4$ band) show an agreement better than 2 % in the 10^{-22}-10^{-21} cm/molecule intensity range, significantly better than our estimated error bar. As expected, a larger dispersion is

observed for the small line intensities, probably with both experimental and theoretical origin. The different bands are distinguishable on the plot. No systematic deviations are evidenced for a particular band indicating that the above-mentioned issue concerning the $\nu_2+3\nu_4$ band is probably unique in the considered region.

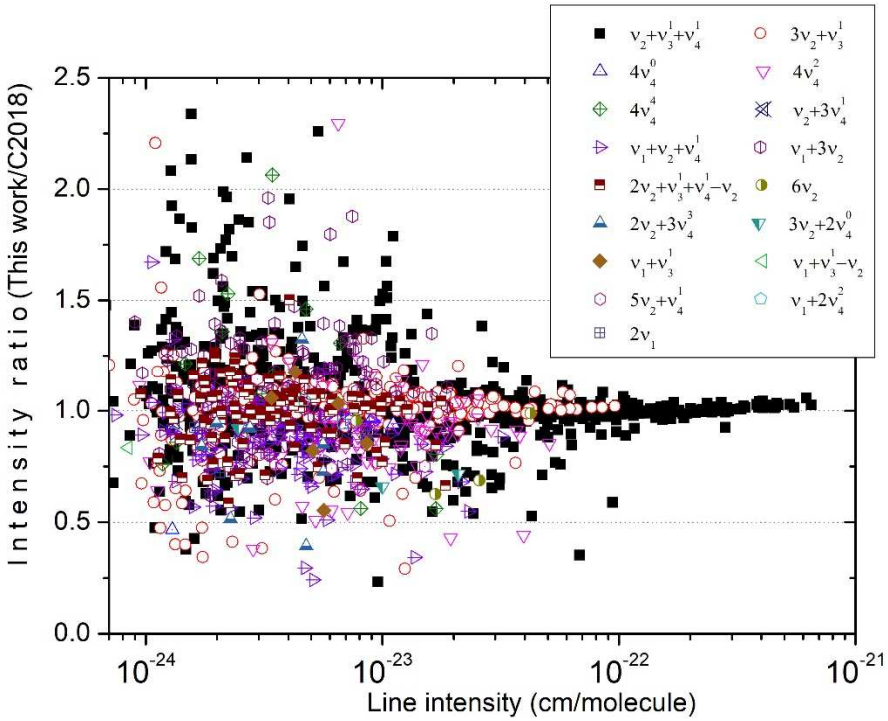

Fig. 7.
Overview of the Exp/C2018 intensity ratios *versus* the FTS line intensity of the $^{14}NH_3$ lines assigned between 5650 and 6350 cm^{-1}.

4. Discussion and concluding remarks

A further instructive comparison can be performed considering the present and HITRAN2016 lists, which overlap in the 6300-6350 cm^{-1} interval (see **Fig. 1**). According to the intensity ratios of the lines in common (**Fig. 8**), our intensity values seem to be systematically smaller by about 10-15 % compared to the HITRAN2016 values. To investigate the origin of this disagreement, we considered the C2018 line list, which shows an average intensity agreement at the % level with our data in the 5650- 6350 cm^{-1} region (**Fig. 7**). The C2018 intensities being validated in our region, we compared the HITRAN2016 intensities to C2018 values in the range extending between 6350 and 6600 cm^{-1}. An attempt was performed to associate the HITRAN and corresponding C2018 transitions using the rovibrational assignment. This was not straightforward, due to the differences in quantum number labelling between C2018 and HITRAN lists. As a consequence, manual verification of each assignment was necessary to pair the transitions.

From the 408 assigned HITRAN lines in the range 6350 and 6600 cm^{-1}, we were able to associate only 357 with a C2018 transition. For 329 transitions, the *J, K* and inversion parity are the

same for lower and upper states, but for 59 of them the vibrational description is not the same (more often $\nu_3+2\nu_4$ is replaced by $\nu_1+\nu_3$) and few discrepancies occurs also on the symmetry description. The resulting HITRAN2016/C2018 intensity ratios are plotted *versus* the line intensities in **Fig. 8**. Over the 6350-6600 cm^{-1} interval, the HITRAN2016 intensity values show a clear tendency to be larger than C2018 values by an amount similar to that obtained compared to our data in the 6300-6350 cm^{-1} interval. Relying on the C2018 absolute intensities, this observation seems to indicate that HITRAN2016 intensity values originating from Ref. [6] are overestimated by about 10% in the region. Note that, according to **Fig. 8**, the dispersion of the intensity ratios is significantly lower for our data than for HITRAN2016 intensities. Finally, let us mention that the intensities of Ref. [6] were found on average about 4% larger than measured in Ref. [9]. Nevertheless, we cannot totally exclude a similar 10% bias for both C2018 and our FTS intensity values in our region.

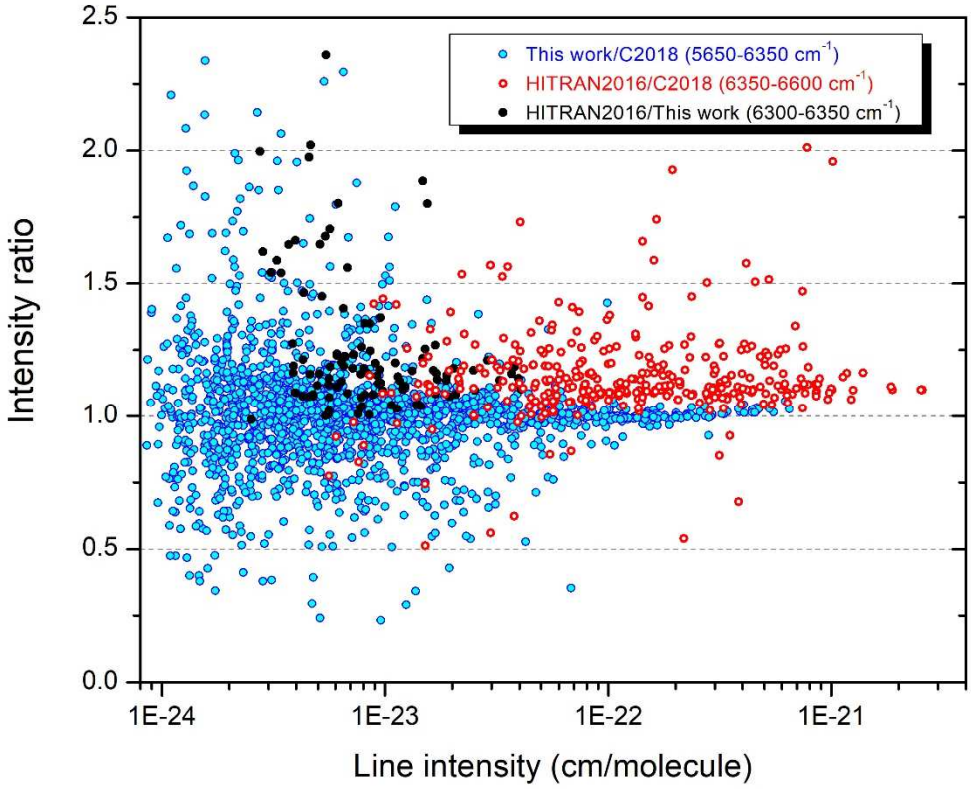

Fig. 8.
Overview of the intensity ratios for $^{14}NH_3$. The comparison to the C2018 list [18] applies to the present measurements between 5650 and 6350 cm^{-1} (blue) and to HITRAN2016 intensities in the 6350-6600 cm^{-1} interval (red). The comparison of our and HITRAN2016 values in the 6300-6350 cm^{-1} common interval (black) is also presented.

Finally, our results were compared to the very recent line lists reported by Beale et al. [14]. These authors constructed several line lists at various temperatures (293-900 K at 100 K intervals) and two pressures (10 and 100 Torr) for the wide 4800-9000 cm^{-1} region. The spectra were recorded by FTS with a 0.01 cm^{-1} resolution and

50.8 m absorption path length. We considered in details the 293 K line lists at 10 and 100 Torr of Ref. [14] and noted some important differences between the line intensities reported at these two pressures. We performed a detailed comparison with our data and found that, although a good general agreement is achieved for both line positions and line intensities, the accuracy of line parameters reported by Beale et al. is not at the level of the present results. The intensity comparison presented in **Fig. 9** with the same scales as in **Fig. 8** illustrates the large uncertainties of the intensities reported in Ref. [14], in particular for the 100 Torr values.

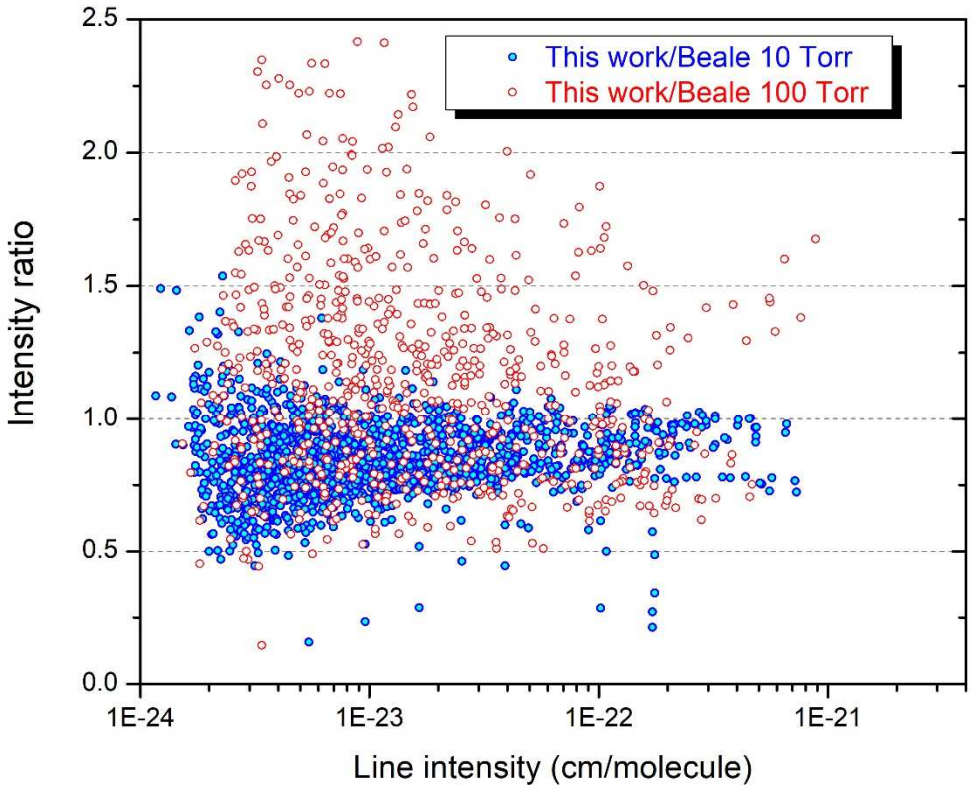

Fig. 9.

Overview of the intensity ratios for NH_3 between 5650 and 6350 cm^{-1} between our values and those retrieved in Ref. [14] at 10 and 100 Torr (blue and red symbols, respectively).

In summary, the 5650 - 6350 cm^{-1} energy range of the ammonia spectrum has been studied using an FTS absorption spectrum recorded at Kitt Peak National Solar Observatory. A total of 2779 lines were measured, and 1762 of them, representing 96% of the absorption in the region, were assigned by the systematic use of LSCD relations and of *ab initio* variational calculation (C2018 list [18] and EXOMOL project www.exomol.com). From these data, 916 energy term values of 29 upper vibrational states were derived. All but two of them are newly reported. The set of derived energy levels will be valuable to correct the variational positions of the C2018 or CoYuTe line lists and

provide them experimental accuracy (about 0.002 cm^{-1}). In the absence of correction, the variational line positions were observed to show deviations up to 1 cm^{-1}. We note that overall, an excellent intensity agreement is achieved between our FTS values and C2018 values. Only one band, namely the $\nu_2+3\nu_4$ pure bending band, was found to have largely overestimated calculated band intensity.

As indicated in the introduction, the present work has been motivated by the lack of data for ammonia in the 1.6 μm atmospheric window. The reported ammonia line list derived from a 30-year-old FTS spectrum could be nowadays significantly improved using higher quality spectra. In the future, we plan to use modern laser spectroscopy methods to improve the ammonia spectroscopy in the region in terms of sensitivity and accuracy of the line centers and line intensities.

Acknowledgements

This work is a contribution of the CPER research project CLIMIBIO. The authors thank the French Ministère de l'Enseignement Supérieur et de la Recherche, the Hauts de France Region and the European Funds for Regional Economic Development for their financial support to this project. This work was also supported by the joint Slovak-Czech-French Danube Region project (DS-FR-19-0050), and by the Slovak Research and Development Agency (contract number APVV-17-0382).

References

[1] Leshchishina O, Mikhailenko SN, Mondelain D, Kassi S, Campargue A. An improved line list for water vapor in the 1.5μm transparency window by highly sensitive CRDS between 5852 and 6607cm^{-1}. J Quant Spectrosc Radiat Transf 2013;130:69–80. doi:10.1016/j.jqsrt.2013.04.010.

[2] Mikhailenko SN, Mondelain D, Karlovets EV, Kassi S, Campargue A. Cavity ring down spectroscopy of 17O enriched water vapor near 1.73 μm. J Quant Spectrosc Radiat Transf 2019;222–223:229–35. doi:10.1016/j.jqsrt.2018.10.027.

[3] Vasilchenko S, Tran H, Mondelain D, Kassi S, Campargue A. Accurate absorption spectroscopy of water vapor near 1.64 μm in support of the MEthane Remote LIdar missioN (MERLIN). J Quant Spectrosc Radiat Transf 2019;235:332–42. doi:10.1016/j.jqsrt.2019.06.027.

[4] Gordon IE, Rothman LS, Hill C, Kochanov RV, Tan Y, Bernath PF, et al. The HITRAN2016 Molecular Spectroscopic Database. J Quant Spectrosc Radiat Transf 2017. doi:10.1016/j.jqsrt.2017.06.038.

[5] Brown LR, Margolis JS. Empirical line parameters of NH_3 from 4791 to 5294 cm^{-1}. J Quant Spectrosc Radiat Transf 1996;56:283–94. doi:10.1016/0022-4073(96)00041-6.

[6] Sung K, Brown LR, Huang X, Schwenke DW, Lee TJ, Coy SL, et al. Extended line positions, intensities, empirical lower state energies and quantum assignments of NH_3 from 6300 to 7000 cm^{-1}. J Quant Spectrosc Radiat Transf 2012;113:1066–83. doi:10.1016/j.jqsrt.2012.02.037.

[7] Barton EJ, Yurchenko SN, Tennyson J, Béguier S, Campargue A. A near infrared line list for NH_3 : Analysis of a Kitt Peak spectrum after 35 years. J Mol Spectrosc 2016;325:7–12. doi:10.1016/j.jms.2016.05.001.

[8] Barton EJ, Yurchenko SN, Tennyson J, Clausen S, Fateev A. High-resolution absorption measurements of NH 3 at high temperatures: 2100–5500 cm^{-1}. J Quant Spectrosc Radiat Transf 2017;189:60–5. doi:10.1016/j.jqsrt.2016.11.009.

[9] Vander Auwera J, Vanfleteren T. Line positions and intensities in the 7400–8600 cm^{-1} region of the ammonia spectrum. Mol Phys 2018;116:3621–30. doi:10.1080/00268976.2018.1467054.

[10] Cacciani P, Čermák P, Cosléou J, Khelkhal M, Jeseck P, Michaut X. New progress in spectroscopy of ammonia in the infrared 1.5μm range using evolution of spectra from 300 K down to 122 K. J Quant Spectrosc Radiat Transf 2012;113:1084–91. doi:10.1016/j.jqsrt.2012.02.026.

[11] Cacciani P, Čermák P, Cosléou J, Romh J El, Hovorka J, Khelkhal M. Spectroscopy of ammonia in the range 6626–6805 cm^{-1} : using temperature dependence towards a complete list of lower state energy transitions. Mol Phys 2014;112:2476–85. doi:10.1080/00268976.2014.924653.

[12] Földes T, Golebiowski D, Herman M, Softley TP, Di Lonardo G, Fusina L. Low-temperature high-resolution absorption spectrum of $^{14}NH_3$ in the $\nu_1+\nu_3$ band region (1.51 μm). Mol Phys 2014;112:2407–18. doi:10.1080/00268976.2014.904944.

[13] Svoboda V, Rakovský J, Votava O. New insight on ammonia 1.5 μm overtone spectra from two-temperature analysis in supersonic jet. J Quant Spectrosc Radiat Transf 2019;227:201–10. doi:10.1016/j.jqsrt.2019.01.030.

[14] Beale CA, Wong A, Bernath P. Infrared transmission spectra of hot ammonia in the 4800–9000 cm^{-1} region. J Quant Spectrosc Radiat Transf 2020;246:106911. doi:10.1016/j.jqsrt.2020.106911.

[15] Huang X, Schwenke DW, Lee TJ. Rovibrational spectra of ammonia. I. Unprecedented accuracy of a potential energy surface used with nonadiabatic corrections. J Chem Phys 2011;134:044320. doi:10.1063/1.3541351.

[16] Huang X, Schwenke DW, Lee TJ. Rovibrational spectra of ammonia. II. Detailed analysis, comparison, and prediction of spectroscopic assignments for $^{14}NH_3$, $^{15}NH_3$, and $^{14}ND_3$. J Chem Phys 2011. doi:10.1063/1.3541352.

[17] Yurchenko SN, Barber RJ, Tennyson J. A variationally computed line list for hot NH_3. Mon Not R Astron Soc 2011;413:1828–34. doi:10.1111/j.1365-2966.2011.18261.x.

[18] Coles PA, Ovsyannikov RI, Polyansky OL, Yurchenko SN, Tennyson J. Improved potential energy surface and spectral assignments for ammonia in the near-infrared region. J Quant Spectrosc Radiat Transf 2018;219:199–212. doi:10.1016/j.jqsrt.2018.07.022.

[19] Al Derzi AR, Furtenbacher T, Tennyson J, Yurchenko SN, Császár AG. MARVEL analysis of the measured high-resolution spectra of $^{14}NH_3$. J Quant Spectrosc Radiat Transf 2015;161:117–30. doi:10.1016/j.jqsrt.2015.03.034.

[20] Furtenbacher T, Coles PA, Tennyson J, Yurchenko SN, Yu S, Drouin B, et al. Empirical rovibrational energy levels of ammonia up to 7500 cm^{-1}. J Quant Spectrosc Radiat Transf 2020;251:107027. doi:10.1016/j.jqsrt.2020.107027.

[21] Coles PA, Yurchenko SN, Tennyson J. ExoMol molecular line lists – XXXV. A rotation-vibration line list for hot ammonia. Mon Not R Astron Soc 2019;490:4638–47. doi:10.1093/mnras/stz2778.

[22] Béguier S, Liu AW, Campargue A. An empirical line list for methane near 1 μm (9028–10,435cm^{-1}). J Quant Spectrosc Radiat Transf 2015;166:6–12. doi:10.1016/j.jqsrt.2015.07.003.

[23] Cacciani P, Cosléou J, Khelkhal M, Tudorie M, Puzzarini C, Pracna P. Nuclear spin conversion in NH3. Phys Rev A 2009;80:042507. doi:10.1103/PhysRevA.80.042507.

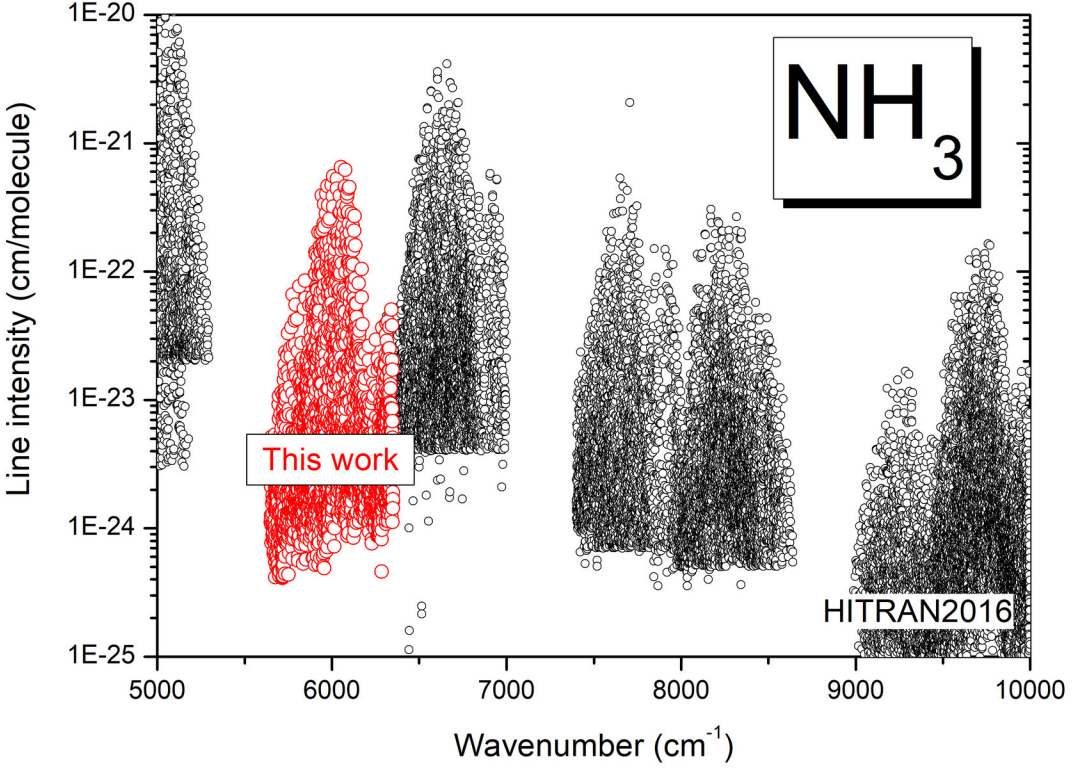
NH3
This work
HITRAN2016
Line intensity (cm/molecule)
1E-20
1E-21
1E-22
1E-23
1E-24
1E-25
5000
6000
7000
8000
9000
10000
Wavenumber (cm-1)